Journal of Power Sources 220 (2012) 354–359

Contents lists available at SciVerse ScienceDirect

Journal of Power Sources

journal homepage: www.elsevier.com/locate/jpowsour

Improved Co-substituted, $LiNi_{0.5-x}Co_{2x}Mn_{1.5-x}O_4$ lithium ion battery cathode materials

Min-Woo Jang [a], Hun-Gi Jung [a], Bruno Scrosati [a,c,*], Yang-Kook Sun [a,b,**]

[a] Department of WCU Energy Engineering, Hanyang University, Seoul 133-791, Republic of Korea
[b] Department of Chemical Engineering, Hanyang University, Seoul 133-791, Republic of Korea
[c] Department of Chemistry, University of Rome Sapienza, Piazzle Aldo Moro 5, 00185 Rome, Italy

HIGHLIGHTS

► Stabilized lithium manganese spinel.
► High performance cathode material.
► Impact in the lithium battery technology.

ARTICLE INFO

Article history:
Received 26 March 2012
Received in revised form
25 July 2012
Accepted 31 July 2012
Available online 8 August 2012

Keywords:
Rate capability
5 V spinel
Cathode
Co substitution
Lithium batteries

ABSTRACT

The synthesis and the structural and morphological characterization of micro-sized, spherical $LiNi_{0.5-x}Co_{2x}Mn_{1.5-x}O_4$ powders are reported. The results demonstrate that these materials have a high electronic conductivity as well as a high tap density. We show that when tested in a lithium cell the Co-substituted $LiNi_{0.5-x}Co_{2x}Mn_{1.5-x}O_4$ electrodes exhibited a better cycling performance and a better rate capability than the Co-free $LiNi_{0.5}Mn_{1.5}O_4$ parent cells. The enhanced electrochemical performances are attributed to the increase in electrical conductivity and in structural stability caused by Co substitution for Ni and Mn and the mixed valence effect of Mn^{3+}/Mn^{4+}. Due to these properties, the $LiNi_{0.5-x}Co_{2x}Mn_{1.5-x}O_4$ electrodes are believed to be of importance for the progress of the lithium battery technology.

1. Introduction

Considerable attention has recently been paid to the development of Li ion batteries with high energy densities and high power capabilities for portable electronic devices and electric vehicles. Energy density is a key factor in lithium batteries; its value can be increased by using cathode materials capable to operate at high capacity and high voltage. Relevant examples of high voltage cathode materials are $LiM_xMn_{2-x}O_4$ (M = Ni, Cr, Fe, Co, Cu, Ti, Mo, etc...), i.e., the so-called 5 V spinels [1–9]. The operating voltage of these materials varies around 4.7–4.9 V depending on the type and the concentration of the doping, transition metal M.

As known, due to its high flat discharge voltage of 4.7 V, nickel substituted $LiNi_{0.5}Mn_{1.5}O_4$ is the most attractive of the family [2,10]. During cycling of $LiNi_{0.5}Mn_{1.5}O_4$, Ni ions are reversibly oxidized and reduced passing from Ni^{2+} to Ni^{4+} with no change in the structure whose stability is assured by the hosted Mn^{4+} ions which remain electrochemically inactive during the electrochemical process [2].

The commercialization of $LiNi_{0.5}Mn_{1.5}O_4$ however, is hindered by a number of still unsolved performance issues mainly resulting in limitations in cycle life, due to side reactions with electrolytes, and in rate capability, caused by the two-step phase transition during cycling. It has in fact been reported that the capacity fade upon cycling of $LiNi_{0.5}Mn_{1.5}O_4$ is mainly due to surface degradation occurring at the electrolyte interface at the high operating voltage of ~5 V [11–13], while the rate capability is controlled by strain occurring during cycling and originating from the two-step phase transitions between three cubic phases [14].

* Corresponding author. Department of Chemistry, University of Rome Sapienza, Piazzle Aldo Moro 5, 00185 Rome, Italy. Tel.: +82 2 2220 0524; fax: +82 2 2282 7329.
** Corresponding author. Department of WCU Energy Engineering, Hanyang University, Seoul 133-791, Republic of Korea. Tel.: +82 2 2220 0524; fax: +82 2 2282 7329.
E-mail addresses: Bruno.Scrosati@uniroma1.it (B. Scrosati), yksun@hanyang.ac.kr (Y.-K. Sun).

0378-7753/$ – see front matter © 2012 Elsevier B.V. All rights reserved.
http://dx.doi.org/10.1016/j.jpowsour.2012.07.104

Surface modification with metal oxides [11–13,15–17], and BiOF [18] is an effective tool for improving electrochemical performances of the spinel since the oxide protects the material surface from electrolyte decomposition as well as from HF attack. The substitution of other metals (M = Li, Mg, Ti, Cr, Fe, Co, Zn, and Mo) for Ni or/and Mn sites in $LiNi_{0.5}Mn_{1.5}O_4$ is another successful approach [9,17,19–21] since most of the substituents improve the electrochemical performances by controlling the lattice parameter variation [19–21] originating from phase transitions. The substituents also improve the electronic conductivity of the spinel [22].

Investigations of cobalt stabilized $LiNi_{0.45}Co_{0.1}Mn_{1.45}O_4$ have been previously reported by one of our laboratories [23,24]. The results showed that this material behaves as a very efficient cathode in novel types of lithium ion batteries based on its combination with a stable, high performance Sn-C anode [23] and with a morphologically optimized $Li_4Ti_5O_{12}$ anode [24],

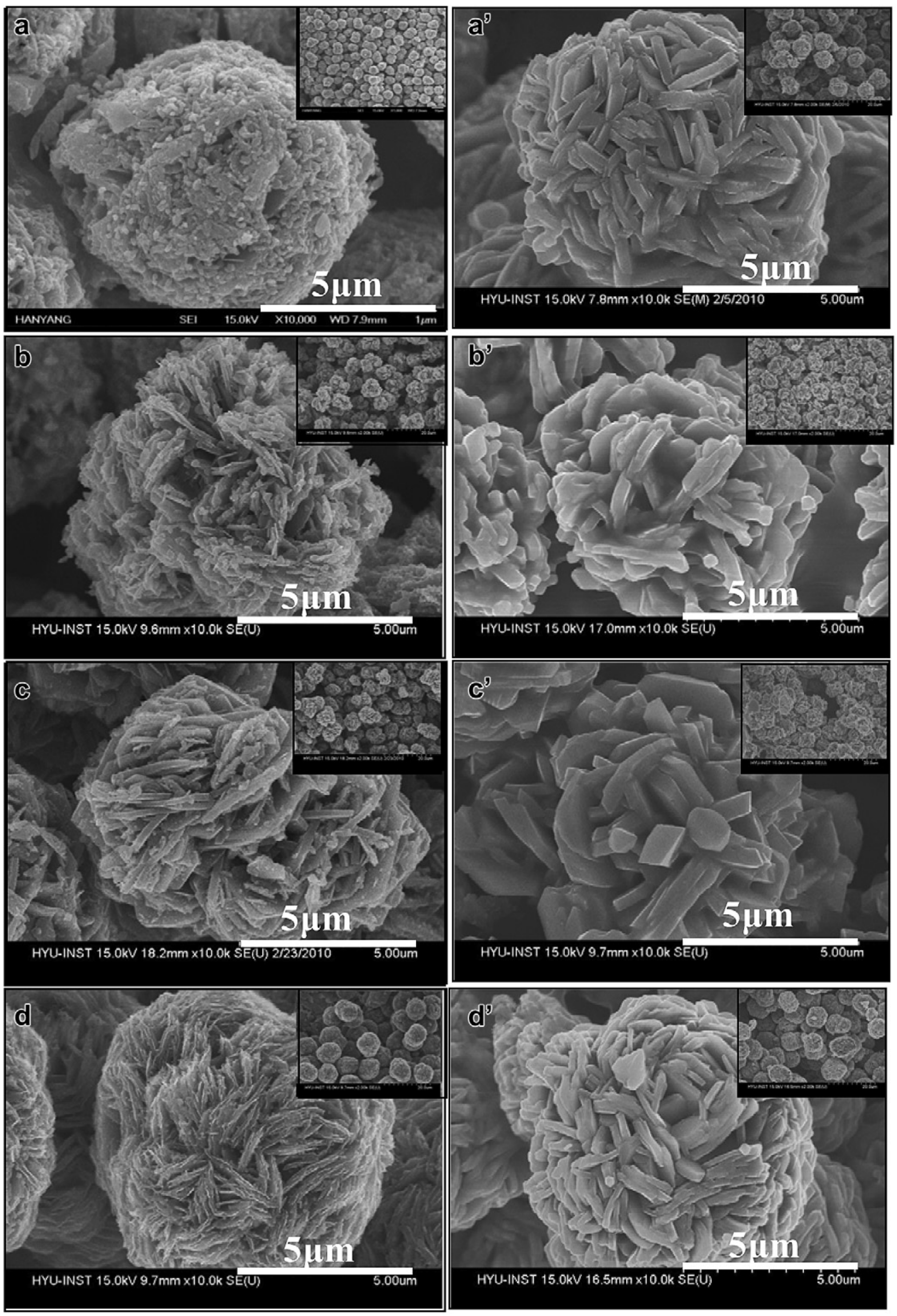

Fig. 1. SEM images of the $[Ni_{0.25-x}Co_xMn_{0.75-x}](OH)_2$ precursors with x values of (a) 0.0, (b) 0.025, (c) 0.05, and (d) 0.075, and of $LiNi_{0.5-x}Co_{2x}Mn_{1.5-x}O_4$ powders with x values of (a′) 0.0, (b′) 0.025, (c′) 0.05, and (d′) 0.075.

respectively. However, to-date there have been no systematic studies of the role of Co in $LiNi_{0.45}Co_{0.1}Mn_{1.45}O_4$. In this work we attempt to fill this gap by evaluating the effects of Co content (x) on the structural and electrochemical properties of $LiNi_{0.5-x}Co_{2x}Mn_{1.5-x}O_4$ ($x = 0.0 \sim 0.075$).

2. Experimental

To synthesize $LiNi_{0.5-x}Co_{2x}Mn_{1.5-x}O_4$ ($x = 0.0 \sim 0.075$), spherical precursors $[Ni_{0.25-x}Co_xMn_{0.75-x}](OH)_2$ (x = 0, 0.025, 0.05, and 0.075) were first prepared by a co-precipitation method [25]. An aqueous solution of $NiSO_4 \cdot 6H_2O$, $CoSO_4 \cdot 6H_2O$, and $MnSO_4 \cdot 5H_2O$ with the desired composition at a concentration of 2.0 mol L^{-1} was pumped into a continuously stirred tank reactor (CSTR, 4 L) under a nitrogen atmosphere. At the same time, a 4.0 mol L^{-1} NaOH solution (aq.) and the desired amount of a NH_4OH solution (aq.) chelating agent were separately fed into the CSTR reactor. The so obtained precursors were filtered and washed with distilled water and then dried at 110 °C for 12 h. The dried powders were thoroughly mixed with Li_2CO_3 (molar ratio of Li/transition metals = 1.02) and calcined at 850 °C for 20 h in air.

Powder X-ray diffraction (XRD, Rint-2000, Rigaku) using Cu-Kα radiation was utilized to identify the crystal structure of the synthesized materials. The morphologies of the powders were evaluated using a scanning electron microscope (SEM, JSM-6340F, JEOL). The chemical compositions of the resulting powders were determined by atomic absorption spectroscopy (AAS, Analyst 300, Perkin Elmer). The DC electrical conductivity was measured by a direct volt–ampere method (CMT-SR1000, AIT Co.) in which disk samples were contacted with a four-point probe.

Electrochemical testing was performed in R2032 coin-type cells. The positive electrodes were fabricated by blending the prepared powders, Super P carbon black, and polyvinylidene fluoride (85:7.5:7.5) in *N*-methyl-2-pyrrolidone. The slurry was then cast on aluminum foil and dried at 110 °C for 10 h in a vacuum oven. The negative electrode was lithium foil and the electrolyte was a 1.2 M $LiPF_6$ solution in an ethylene carbonate (EC)-ethyl methyl carbonate (EMC) mixture (3:7 ratio by volume, PANAX ETEC Co., Ltd., Korea). The positive and negative electrodes were separated by a porous polypropylene film.

3. Results and discussion

To obtain micro-sized, spherical, high tap density $LiNi_{0.5-x}Co_{2x}Mn_{1.5-x}O_4$ ($x = 0.0 \sim 0.075$) powders we used a dense spherical $[Ni_{0.25-x}Co_xMn_{0.75-x}](OH)_2$ hydroxide precursor. Fig. 1 shows SEM images of the $[Ni_{0.25-x}Co_xMn_{0.75-x}](OH)_2$ ($x = 0 \sim 0.075$) precursor and of its corresponding lithiated oxides, $LiNi_{0.5-x}Co_{2x}Mn_{1.5-x}O_4$ ($x = 0 \sim 0.075$). All of the particles are spherical and the diameter of both the precursors and the lithiated oxides is estimated to be 7 μm. As expected [25], the spherical morphology and the particle diameter of the lithiated oxides remained unchanged after high temperature calcination. The thicknesses of the needle-shaped primary particles in the precursors increased with increasing Co-substitution amount up to x = 0.05 and then decreased. A similar behavior is observed in the corresponding lithiated oxide primary particles, where the bar-like shape gradually changed to an octahedron-like shape, resulting in a progressive increase in tap density as confirmed by Table 1 that reports the values of this parameter for both the precursor and the lithiated oxides $LiNi_{0.5-x}Co_{2x}Mn_{1.5-x}O_4$ ($x = 0.0 \sim 0.075$) as a function of Co content. Clearly, the highest tap density, i.e., 2.2 g cc^{-1}, is provided by the materials with x = 0.05 and 0.075, i.e., with the highest cobalt concentration.

Table 1
Tap density of the $[Ni_{0.25-x}Co_xMn_{0.75-x}](OH)_2$ precursor and of the lithiated oxide, $Li[Ni_{0.5-x}Co_{2x}Mn_{1.5-x}]O_4$ as function of the Co content.

x	0.0 g cc^{-1}	0.025 g cc^{-1}	0.05 g cc^{-1}	0.075 g cc^{-1}
Precursor	1.4	1.5	1.6	1.6
Lithiated oxide	1.9	2.0	2.2	2.2

Fig. 2 shows the XRD patterns of the $LiNi_{0.5-x}Co_{2x}Mn_{1.5-x}O_4$ ($x = 0.0 \sim 0.075$) powder samples; the spectra reveals that all of them have a well defined spinel phase with a *Fd3m* space group. The pure $Li[Ni_{0.5}Mn_{1.5}]O_4$ phase is difficult to obtain because of the Ni solubility; formations of impurity phases, such NiO and $Li_{1-x}Ni_xO$, are in fact often observed for this material [2,26,27]. However, no Co impurities or Ni-related phases were observed in our $LiNi_{0.5-x}Co_{2x}Mn_{1.5-x}O_4$ samples.

The lattice parameters of the samples were calculated by a least squares method using the XRD data. Fig. 3 shows the results: as the Co content (x) increases, the lattice parameter a linearly decreases from 8.179 Å (x = 0.0) to 8.168 Å (x = 0.075), indicating that the Co^{3+} ions are uniformly distributed in the Ni^{2+} and Mn^{4+} octahedral sites. The decrease of the a lattice parameter may be due to substitution of the smaller Co^{3+} (0.53 Å) ion for the larger Ni^{2+} (0.76 Å) and Mn^{4+} (0.54 Å) ions [28]. We suggest that the linear variation in the lattice parameter a as a function of the Co content implies a successful formation of a solid solution in $LiNi_{0.5-x}Co_{2x}Mn_{1.5-x}O_4$, obeying Vegard's rule.

Table 2 shows the electrical conductivity of the $LiNi_{0.5-x}Co_{2x}Mn_{1.5-x}O_4$ ($x = 0.0 \sim 0.075$) samples here under study. The conductivity increases by increasing the Co content (x), to reach a maximum value of 6.46×10^{-6} S cm^{-1} for the $LiNi_{0.4}Co_{0.1}Mn_{1.4}O_4$ sample, which is 3 times higher than that of Co-free $LiNi_{0.5}Mn_{1.5}O_4$, (1.91×10^{-6} S cm^{-1}). It is believed that the increase in conductivity is due to the Mn^{3+}/Mn^{4+} mixed valence effect promoted by the larger Mn^{3+} concentration resulting from the high Co substitution [29].

Fig. 4 shows the first charge/discharge curves of the $Li/LiNi_{0.5-x}Co_{2x}Mn_{1.5-x}O_4$ ($x = 0.0 \sim 0.075$) materials cycled in a lithium cell between 3.5 and 4.9 V voltage limits and at a current density of 24 mA g^{-1} (0.2 °C-rate). The cell exhibited a long, flat 4.7 V plateau followed by a much shorter 4.0 V plateau; the former is attributed to the Ni^{2+}/Ni^{4+} redox process and the latter to the Mn^{3+}/Mn^{4+} redox process [2,30,31]. The length of this second plateau increases by increasing the Co fraction, reaching the highest value for a Co content of 0.1 (x = 0.05). This trend can be accounted for by considering that an increase in Co content results in an

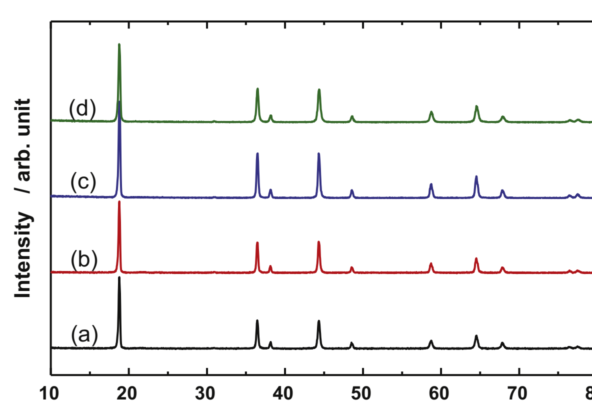

Fig. 2. X-ray diffraction patterns of $LiNi_{0.5-x}Co_{2x}Mn_{1.5-x}O_4$ powders with x values of (a) 0.0, (b) 0.025, (c) 0.05, and (d) 0.075.

Table 2
Electrical conductivity of $Li[Ni_{0.5-x}Co_{2x}Mn_{1.5-x}]O_4$ samples as function of the Co content.

Sample	Electrical conductivity ($S\ cm^{-1}$)
$LiNi_{0.5}Mn_{1.5}O_4$	1.91×10^{-6}
$LiNi_{0.475}Co_{0.05}Mn_{1.475}O_4$	2.51×10^{-6}
$LiNi_{0.45}Co_{0.1}Mn_{1.45}O_4$	6.46×10^{-6}
$LiNi_{0.425}Co_{0.15}Mn_{1.425}O_4$	3.92×10^{-6}

increase of Mn^{3+} concentration. On the other hand, Fig. 4 also reveals that the increase in Co reflects in a gradual decrease in the value of the discharge capacity. We hypothesize that this effect is due to the impoverishment of the electro-active Ni^{2+}; we can in fact exclude a role of the substituent Co since its electrochemical response, associate with the Co^{3+}/Co^{4+} redox process, is expect to occur at 5.1 V [4,6].

To evidence the variation of the voltage profiles around 4.7 V, the initial charge and discharge curves of the $Li/LiNi_{0.5-x}Co_{2x}Mn_{1.5-x}O_4$ cells reported in Fig. 4 were differentiated and the results are shown in Fig. 5. Two distinct peaks were observed at 4.7 and 4.75 V in the charge voltage profile of the $Li/LiNi_{0.5}Mn_{1.5}O_4$ ($x = 0$) cell. As the Co content increases, the upper plateau (Ni^{3+}/Ni^{4+} redox) is shifted to progressively higher voltages, contrary to the behavior of the lower plateau arising from the Ni^{2+}/Ni^{3+} redox that moves to lower voltages showing clear broadening of the peaks. The shift to high voltage following the increase in Co content may be associated with a change of the bonding strength of the substituted spinel structure. We hypothesized that similar phenomena are due to difference in Gibbs free energies of formation of the constituent oxides [8], being at 298 K for NiO, Co_2O_3, and MnO_2 equal to -211.7 kJ mol^{-1}, -560 kJ mol^{-1}, and -465.2 kJ mol^{-1}, respectively, suggesting that the Co–O bond is stronger than both Ni–O and Mn–O bonds [32]. We believe that an increase in strength of the Co–O bonding may lead to an increase in the redox potential.

Fig. 6a shows the cycling performance of the $Li/LiNi_{0.5-x}Co_{2x}Mn_{1.5-x}O_4$($x = 0.0\sim0.075$) cells cycled between 3.5 and 4.9 V at 25 °C under a specific current density of 60 mA g^{-1} (0.5 °C-rate). This is the highest initial discharge capacity i.e., 136 mAh g^{-1} is shown by the $LiNi_{0.5}Mn_{1.5}O_4$ ($x = 0$)-based cell; however this cell also shows a poor capacity retention, i.e., 90.8% after 100 cycles, while the cells using the Co substituted electrodes, although having a lower initial capacity, have a much more stable

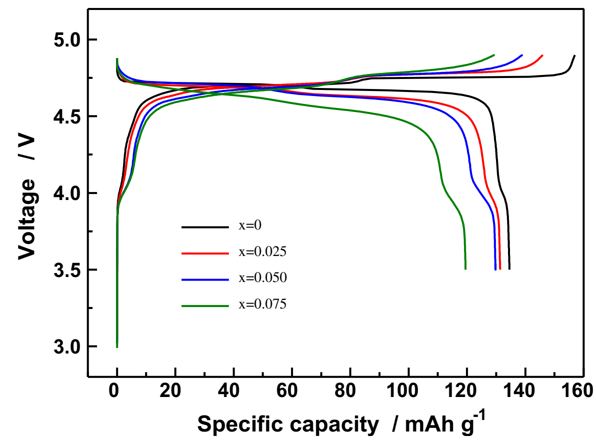

Fig. 4. Initial charge/discharge curves of the $Li/LiNi_{0.5-x}Co_{2x}Mn_{1.5-x}O_4$ cells ($x = 0.0\sim0.075$) cycled between 3.5 and 4.9 V at a current density of 24 mA g^{-1} (0.2 °C-rate).

capacity retention, i.e., capacity retention of 96.4% ($x = 0.025$), 97.2% ($x = 0.050$) and 99% ($x = 0.075$).

To further test the role of the Co content on their cycling performance, the $Li/LiNi_{0.5-x}Co_{2x}Mn_{1.5-x}O_4$ lithium cells were tested at 55 °C and the results are shown in Fig. 6b. A trend very similar to that obtained at room temperature was observed, apart from a general increase of the discharge capacity at initial cycling, as expected from the temperature enhanced electronic conductivity of the materials, and some severe capacity decays at the end of the test for the cells with the lowest Co content, probably due to material dissolution. Indeed, the best cycle life with high capacity retention was provided by the cells using the electrodes having the highest cobalt contents, namely by the $Li/LiNi_{0.45}Co_{0.10}Mn_{1.45}O_4$ and by the $Li/LiNi_{0.425}Co_{0.15}Mn_{1.425}O_4$ cells, that kept a capacity retention of 94.9% and of 96.2%, respectively. These results outline the important role of the Co component that, by inducing enhancement in the structural stability deriving by its substitution for Ni and Mn sites, prevents material dissolution, this finally leading to a great improvement in the electrochemical response of the $LiNi_{0.5-x}Co_{2x}Mn_{1.5-x}O_4$ electrodes when cycled in a lithium cell.

Finally, the rate capability of the $LiNi_{0.5-x}Co_{2x}Mn_{1.5-x}O_4$ ($x = 0.0\sim0.075$) electrodes has been determined by discharge tests run under current density progressively increasing from 24 mA g^{-1}

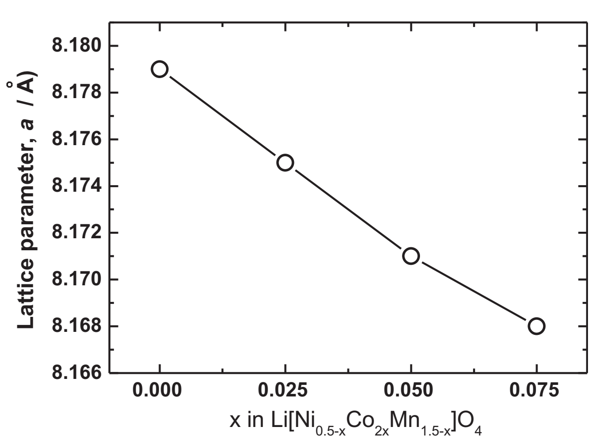

Fig. 3. Variation of the lattice constant a as a function of the Co content, x, in $LiNi_{0.5-x}Co_{2x}Mn_{1.5-x}O_4$.

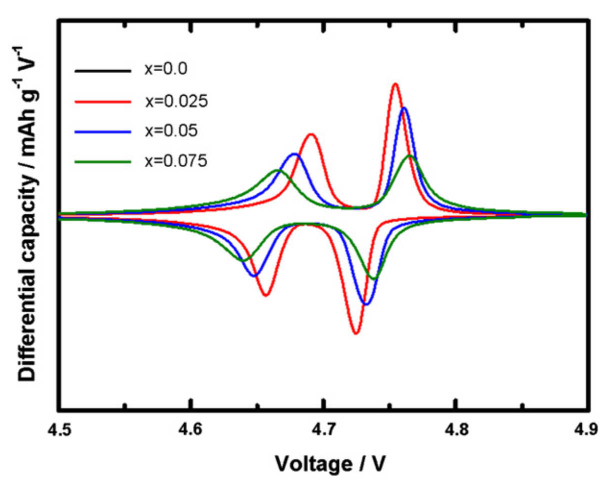

Fig. 5. Differential capacity *vs.* voltage curves for $LiNi_{0.5-x}Co_{2x}Mn_{1.5-x}O_4$ ($x = 0.0$, 0.025, 0.05, and 0.075).

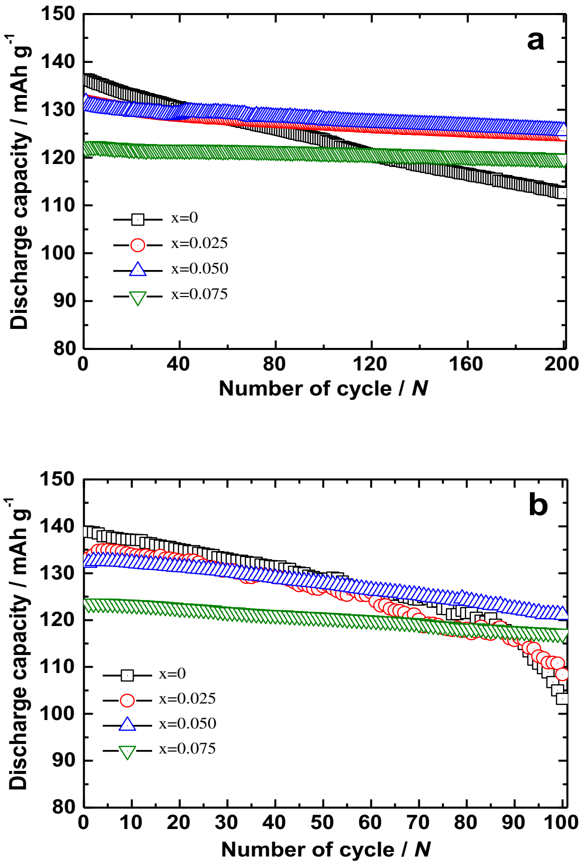

Fig. 6. Discharge capacity *vs.* cycle number of $Li/LiNi_{0.5-x}Co_{2x}Mn_{1.5-x}O_4$ cells ($x = 0.0 \sim 0.075$) cycled between 3.5 and 4.9 V at (a) 25 °C and (b) 55 °C under a current density of 60 mA g^{-1} (0.5 °C).

(0.2 °C) to 2400 mA g^{-1} (20 °C) and between 3.5 and 4.9 V voltage limit. Fig. 7a–d compares the results obtained for the four lithium cells here considered. All cells were charged at the same current density of 24 mA g^{-1} (0.2 °C) before each discharge. At the low discharge rate of 0.5 °C, the cells exhibited a comparable rate capability, namely 137 mAh g^{-1} ($x = 0.0$), 130 mAh g^{-1} ($x = 0.025$), 128 mAh g^{-1} ($x = 0.050$) and 118 mAh g^{-1} ($x = 0.075$), respectively. However, at discharge rates exceeding 10 °C (1200 mA g^{-1}), the Co-substituted $LiNi_{0.5-x}Co_{2x}Mn_{1.5-x}O_4$ cells exhibited a significantly enhanced rate capability. For instance, at a 20 °C-rate (2400 mA g^{-1}) the $LiNi_{0.5}Mn_{1.5}O_4$ cell gave a discharge capacity of only 80.7 mAh g^{-1} with a significant voltage drop to below 4 V, while at the same current rate the other cells had much better capacity retention and voltage profile (compare Fig. 7a with b–d). This dramatic difference may be explained on the basis of the electrical conductivity of the various electrode materials. The, poorly electrode conducting, Co-free $LiNi_{0.5}Mn_{1.5}O_4$ cell is affected by severe polarization. On the other hand, the $LiNi_{0.45}Co_{0.1}Mn_{1.45}O_4$ cell, exploiting the electrode with the highest conductivity of the series (see Table 2) exhibited a discharge capacity of 112.4 mAh g^{-1} with little voltage polarization even at very high current rates (compare Fig. 7c with a).

4. Conclusions

We show in this work that micro-sized spherical shaped $LiNi_{0.5-x}Co_{2x}Mn_{1.5-x}O_4$ ($x = 0.0 \sim 0.75$) electrodes, prepared by the co-precipitation synthesis optimized in our laboratory, show a very promising behavior, in terms of capacity retention, cycle life stability and rate capability, when used as cathodes in lithium cells. We believe that this high electrode performance results from the improved electric conductivity of the electrodes due to the Mn^{3+}/Mn^{4+} mixed valence effect caused by the Co substitution. The results reported in this work outline the important role of the Co substitution for Ni and Mn sites such as enhancing the structural stability and preventing material dissolution. Thus Co substitution

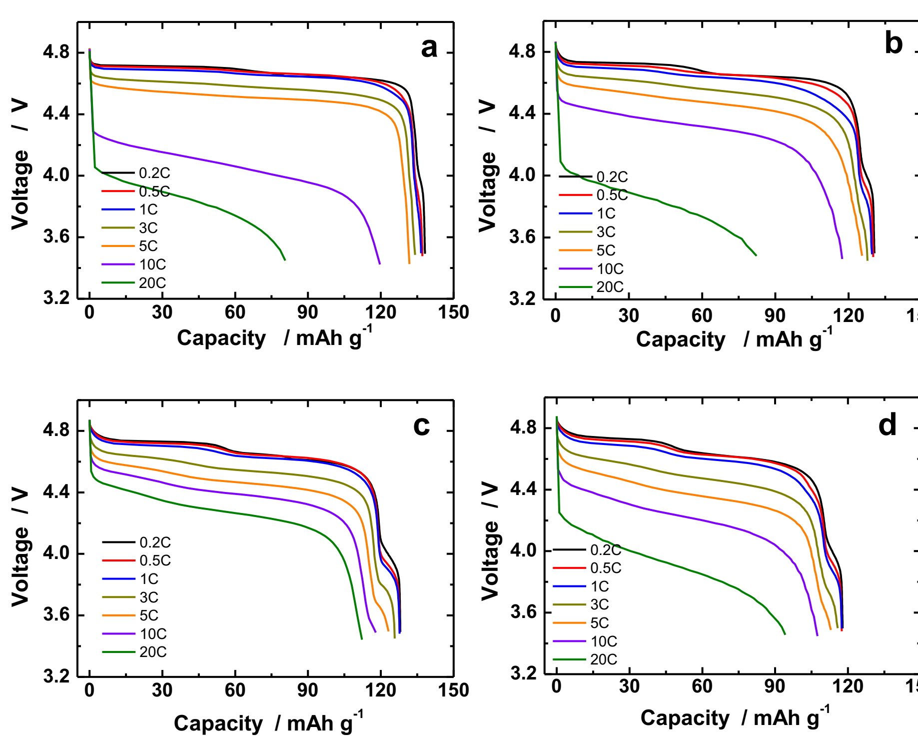

Fig. 7. Rate capabilities of (a) $Li[Ni_{0.5}Mn_{1.5}]O_4$, (b) $LiNi_{0.475}Co_{0.05}Mn_{0.475}O_4$, (c) $LiNi_{0.45}Co_{0.1}Mn_{0.45}O_4$, and (d) $LiNi_{0.425}Co_{0.15}Mn_{0.425}O_4$ between 3.5 and 4.9 V at various currents.

finally leads to a great improvement in the electrochemical performances of the $LiNi_{0.5-x}Co_{2x}Mn_{1.5-x}O_4$ electrodes when cycled in a lithium cell. In addition, these electrode materials benefit to a high tap density, i.e., of the order of 2.2 g cc^{-1}. It is worth to recall here that a high tap density is a quite welcome feature for an electrode since it has a direct reflection of the volumetric energy density of the cell that utilizes it. For all the unique properties above outlined, we believe that the Co-stabilized $LiNi_{0.5-x}Co_{2x}Mn_{1.5-x}O_4$ electrodes may have an important role for the progress of the lithium battery technology.

Acknowledgments

This research was supported by WCU (World Class University) program through the National Research Foundation of Korea funded by the Ministry of Education, Science and Technology (R31-10092).

References

[1] K. Amine, H. Tukamoto, H. Yasuda, Y. Fujita, J. Electrochem. Soc. 143 (1996) 1607.
[2] Q. Zhong, A. Bonakdarpour, M. Zhang, Y. Gao, J.R. Dahn, J. Electrochem. Soc. 144 (1997) 205.
[3] C. Sigala, D. Guyomard, A. Verbaere, Y. Piffard, M. Tournoux, Solid State Ionics 81 (1995) 167.
[4] T. Ohzuku, S. Takeda, M. Iwanaga, J. Power Sources 81 (1999) 90.
[5] H. Kawai, M. Nagata, M. Tabuchi, H. Tukamoto, A.R. West, Chem. Mater. 10 (1998) 3267.
[6] H. Kawai, M. Nagata, H. Tukamoto, A.R. West, J. Mater. Chem. 8 (1998) 837.
[7] P. Strobel, A. Ibarra Palos, M. Anne, F. Le Cras, J. Mater. Chem. 10 (2000) 429.
[8] J.-H. Kim, S.-T. Myung, C.S. Yoon, I.-H. Oh, Y.-K. Sun, J. Electrochem. Soc. 151 (2004) A1911.
[9] S.-H. Park, S.-W. Oh, S.-T. Myung, Y.-K. Sun, Electrochem. Solid State Lett. 7 (2004) A451.
[10] K. Ariyoshi, Y. Iwakoshi, N. Nakayama, T. Ohzuku, J. Electrochem. Soc. 151 (2004) A296.
[11] Y.-K. Sun, K.-J. Hong, J. Prakash, K. Amine, Electrochem. Commun. 4 (2002) 344.
[12] Y.-K. Sun, C.S. Yoon, I.H. Oh, Electrochim. Acta 48 (2003) 503.
[13] R. Alcántara, M. Jaraba, P. Lavela, J.L. Tirado, J. Electronal. Chem. 566 (2004) 187.
[14] J.-H. Kim, S.-T. Myung, C.S. Yoon, S.G. Kang, Y.-K. Sun, Chem. Mater. 16 (2004) 906.
[15] T. Noguchi, I. Yamazaki, T. Numataa, M. Shirakata, J. Power Sources 174 (2007) 359.
[16] J. Liu, A. Manthiram, Chem. Mater. 21 (2009) 1695.
[17] J. Liu, A. Manthiram, J. Electrochem. Soc. 156 (2009) A66.
[18] H.-B. Kang, S.-T. Myung, K. Amine, S.-M. Lee, Y.-K. Sun, J. Power Sources 195 (2010) 2023.
[19] T.A. Arunkumar, A. Manthiram, Electrochem. Solid State Lett. 8 (2005) A403.
[20] S. Mukerjee, X.Q. Yang, X. Sun, S.J. Lee, J. McBreen, Y. Ein-Eli, Electrochim. Acta 49 (2004) 3373.
[21] A. Ito, D. Li, Y. Lee, K. Kobayakawa, Y. Sato, J. Power Sources 185 (2008) 1429.
[22] S.W. Oh, S.-T. Myung, H.B. Kang, Y.-K. Sun, J. Power Sources 189 (2009) 752.
[23] J. Hassoun, K.-S. Lee, Y.-K. Sun, B. Scrosati, J. Am. Chem. Soc. 133 (2011) 3139.
[24] H.-G. Jung, M.W. Jang, J. Hassoun, Y.-K. Sun, B. Scrosati, Nat. Commun. 2 (2011) 516. http://dx.doi.org/10.1038/ncomms1527.
[25] M.-H. Lee, Y.-J. Kang, S.-T. Myung, Y.-K. Sun, Electrochim. Acta 50 (2004) 939.
[26] Y.-K. Sun, Y.-S. Lee, M. Yoshio, K. Amine, Electrochem. Solid State Lett. 5 (2002) A99.
[27] K. Takahashi, M. Saitoh, M. Sano, M. Fujita, K. Kifune, J. Electrochem. Soc. 151 (2004) A173.
[28] J.A. Dean, Lange's Handbook of Chemistry, fourth ed., McGraw-Hill Inc., New York, 1992, pp. 4.13.
[29] G.B. Zhong, Y.Y. Wang, Y.Q. Yu, C.H. Chen, J. Power Sources 205 (2012) 385.
[30] Y. Terada, K. Yasaka, F. Nishikawa, T. Konishi, M. Yoshio, I. Nakai, J. Solid State Chem. 156 (2001) 286.
[31] Y. Idemoto, H. Narai, N. Koura, J. Power Sources 119-121 (2003) 125.
[32] J.A. Dean, Lange's Handbook of Chemistry, fourth ed., McGraw-Hill Inc., New York, 1992, pp. 6.81.